Acta Cryst E
CRYSTALLOGRAPHIC
COMMUNICATIONS

ISSN 2056-9890

Synthesis, crystal structure and Hirshfeld surface analysis of bis[2-amino-5-(ethylsulfanyl)-1,3,4-thiadiazol-3-ium] bis(perchlorato-κO)-bis(picolinato-$\kappa^2 N,O$)copper(II)

Gulnaz Khojabaeva,[a] Batirbay Torambetov,[a,b]* Rajesh G. Gonnade,[c,b] Zamira Uzakbergenova,[d] Abdusamat Rasulov[e] and Shakhnoza Kadirova[a]

[a]National University of Uzbekistan named after Mirzo Ulugbek, 4 University St., Tashkent, 100174, Uzbekistan, [b]Physical and Material Chemistry Division, CSIR-National Chemical Laboratory, Pune, 411008, India, [c]Academy of Scientific and Innovative Research (AcSIR), Sector 19, Kamla Nehru, Nagar, Ghaziabad, Uttar Pradesh 201002, India, [d]Karakalpak State University, 1 Ch. Abdirov St. Nukus, 230112, Uzbekistan, and [e]Termez University of Economics and Service, 41B Farovon St., Termiz, 190111, Uzbekistan. *Correspondence e-mail: torambetov_b@mail.ru

Received 19 May 2025
Accepted 2 June 2025

Edited by B. Therrien, University of Neuchâtel, Switzerland

Keywords: crystal structure; copper(II) complex; picolinate ligand; thiadiazole cation; Hirshfeld surface analysis; hydrogen bonding; supramolecular interactions; Jahn–Teller distortion.

CCDC reference: 2455854

Supporting information: this article has supporting information at journals.iucr.org/e

In the title coordination complex, $(C_4H_8N_3S_2)_2[Cu(C_6H_4NO_2)_2(ClO_4)_2]$, the Cu^{II} center exhibits a distorted octahedral geometry with an equatorial plane formed by two bidentate picolinato ligands and axial coordination from two perchlorate anions, consistent with a Jahn–Teller distortion. The crystal structure is further consolidated by a network of hydrogen bonds involving the thiadiazole-based cations, which reside in the outer coordination sphere in a unique protonated state. Hirshfeld surface analysis reveals that O···H/H···O contacts dominate the intermolecular interactions, contributing significantly to the crystal packing.

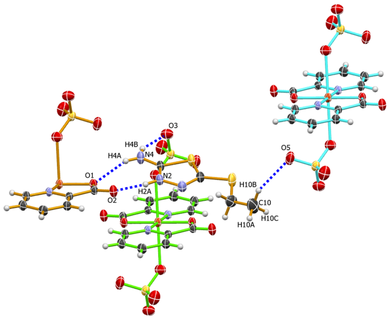

1. Chemical context

The coordination chemistry of transition-metal complexes with heterocyclic ligands has attracted substantial attention because of their diverse applications in catalysis, medicinal chemistry, and materials science. Among such ligands, picolinate anions and 1,3,4-thiadiazole derivatives are especially prominent due to their strong metal-binding abilities and biological relevance. Picolinic acid and its derivatives are well-known for their bidentate coordination modes, often employed in the design of metal–organic complexes to modulate metal center reactivity and bioactivity (Lavrenova *et al.*, 2023). Similarly, 1,3,4-thiadiazole derivatives are recognized for their wide spectrum of biological properties, including antimicrobial, anticancer, and antidiabetic activities (Hu *et al.*, 2014; Gond *et al.*, 2022; Dani *et al.*, 2015). These heterocycles, containing electron-donating nitrogen and sulfur atoms, readily coordinate with transition metals, thereby influencing the physicochemical and pharmacological properties of the resulting complexes (Kadirova *et al.*, 2022; Atashov *et al.*, 2024). Transition metals such as zinc(II), nickel(II), and cobalt(II) have been extensively studied in coordination with thiadiazole-based ligands. Zinc(II) complexes have shown promise in drug delivery and enzyme mimicry (Shen *et al.*, 2004), while nickel(II) and cobalt(II) derivatives exhibit significant catalytic activity and electrochemical potential (Song *et al.*, 2012; Ishankhodzhaeva *et al.*, 2001; Ma *et al.*, 2018; Nuralieva *et al.*, 2025). These findings underscore the versatility of thiadiazole coordination chemistry across various metal centers. Among transition metals,

https://doi.org/10.1107/S2056989025004992

copper(II) occupies a unique position due to its redox flexibility and biological significance. Copper(II) complexes incorporating 1,3,4-thiadiazole ligands have been investigated extensively for their enhanced antimicrobial and anticancer properties compared to the free ligands (Karcz *et al.*, 2020; Heidari *et al.*, 2020). The synergistic effect between the copper center and heterocyclic ligand often leads to improved biological efficacy, making them attractive scaffolds for drug development (Gurbanov *et al.*, 2023; Camí *et al.*, 2005).

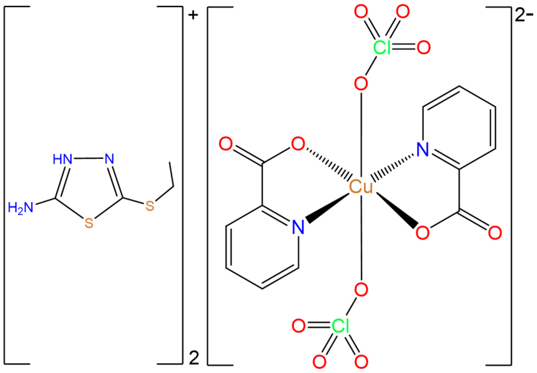

In this context, we present the synthesis, structural characterization, and Hirshfeld surface analysis of the complex $(HL)_2[Cu(Pic)_2(ClO_4)_2]$, where Pic is the picolinate anion and H*L* is the 2-amino-5-ethylthio-1,3,4-thiadiazol-3-ium cation. The structural investigation, carried out using single-crystal X-ray diffraction (SC-XRD), aimed to elucidate the coordination environment, intermolecular interactions, and potential implications for biological activity.

2. Structural commentary

Single-crystal X-ray diffraction analysis reveals that $(HL)_2[Cu(Pic)_2(ClO_4)_2]$ crystallizes in the triclinic $P\overline{1}$ space group. The asymmetric unit consists of half of a Cu^{II} cation, one picolinate anion, one perchlorate anion and one protonated 2-amino-5-ethylthio-1,3,4-thiadiazole (H*L*) ligand. The Cu^{II} cation is positioned on an inversion center and adopts an axially elongated octahedral coordination geometry (Fig. 1). The equatorial plane consists of two nitrogen atoms (N1) and two carboxylate oxygen atoms from symmetry-related picolinate ligands, forming a nearly planar $Cu(pic)_2$ moiety. The axial sites are occupied by two perchlorate anions, each weakly coordinating to the Cu^{II} center. The elongated Cu1—O6 distance of 2.532 (2) Å exceeds the typical Cu—O coordination bond range (1.8–2.0 Å) (Veidis *et al.*, 1969), consistent with a Jahn–Teller distortion along the O6–Cu–O6 axis. The $Cu(Pic)_2$ moiety is nearly planar, with the root-mean-square (r.m.s.) deviations of the oxygen atoms being 0.039 Å for O1 and 0.073 Å for O2, indicating a high degree of planarity in this coordination environment. The geometry and bond lengths of the coordinated picolinato ligands are characteristic of a deprotonated carboxylate group (Fábry, 2018), with the coordinated C—O bond length [1.281 (3) Å] being slightly longer than the C═O bond [1.231 (3) Å].

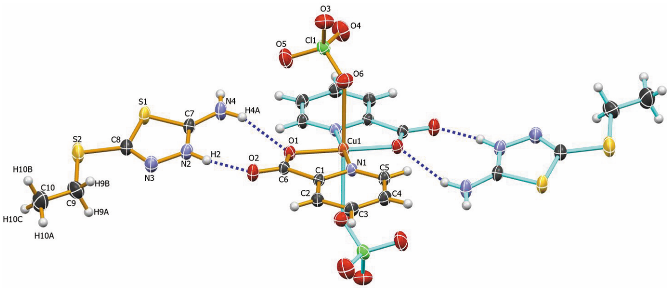

Figure 1
Molecular structure of the title copper(II) complex showing the coordination environment around the Cu^{II} center. Displacement ellipsoids are drawn at the 50% probability level. Hydrogen bonds are indicated by blue dashed lines.

Table 1
Hydrogen-bond geometry (Å, °).

D—H···*A*	*D*—H	H···*A*	*D*···*A*	*D*—H···*A*
N4—H4*A*···O1	0.86	2.14	2.940 (3)	156
N4—H4*A*···O5	0.86	2.59	2.951 (3)	106
N4—H4*B*···O3^{i}	0.86	2.21	2.981 (3)	150
N4—H4*B*···O6^{i}	0.86	2.57	3.005 (3)	113
N2—H2···O2	0.86	1.81	2.656 (3)	170

Symmetry code: (i) $x - 1, y, z$.

3. Supramolecular features

In the extended structure, the $[Cu(pic)_2(ClO_4)_2]^{2-}$ units are assembled into a supramolecular network through hydrogen-bonding interactions with the H*L* protonated thiadiazole cations (Fig. 2, Table 1). The crystal packing is governed by two distinct types of hydrogen bonds: intermolecular and

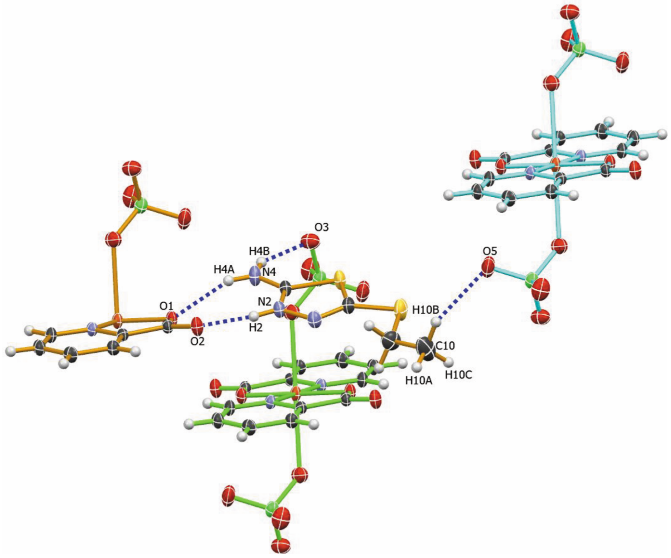

Figure 2
Packing diagram of the title complex showing intermolecular hydrogen bonding (blue dashed lines) between the thiadiazole cation and coordinated perchlorate anions, contributing to the supramolecular architecture. Different molecular fragments are color-coded for clarity. Displacement ellipsoids are drawn at the 50% probability level.

intramolecular. Intermolecular hydrogen bonds are observed between the O3 atom of the perchlorate anion and the amine hydrogen atom of the thiadiazole cation (O3$\cdots$H4*B* = 2.21 Å), as well as between the O5 atom of the perchlorate anion and the hydrogen atom of the methyl group of the thiadiazole cation (O5$\cdots$H10*B* = 2.32 Å). Intramolecular hydrogen bonds occur between the protonated H2*A* atom and atom H4*A* of the thiadiazole ring with carboxylate atoms O2 and O1 in the pic ligands (H2*A*$\cdots$O2 = 1.80 Å, H4*A*$\cdots$O1 = 2.14 Å), forming eight-membered ring motifs with an $R_2^2(8)$ graph set (Bernstein *et al.*, 1995). These non-covalent interactions play a crucial role in the cohesion of the three-dimensional crystal architecture.

4. Hirshfeld Surface Analysis

Hirshfeld surface (HS) analysis was performed and two-dimensional fingerprint (FP) plots were generated using *CrystalExplorer 21.5* (Spackman *et al.*, 2021) to systematically examine the intermolecular interactions governing the crystal packing. In the HS diagram, contacts with interatomic distances equal to the sum of van der Waals radii are represented in white, while those shorter and longer than this threshold appear in red and blue, respectively. The FP plots provide a quantitative assessment of the relative contributions of distinct intermolecular interactions. These plots were generated based on the distances d_e (the distance from the HS to the nearest external atom) and d_i (the distance from the HS to the nearest internal atom). Prior to HS calculations, O—H bond lengths were standardized to neutron diffraction values (0.983 Å) to ensure computational accuracy. HS analysis was conducted separately for the cationic and anionic motifs to delineate their individual contributions to the overall crystal packing. The intermolecular O$\cdots$H/H$\cdots$O interactions were found to be predominant, contributing 22% to the HS area in the thiadiazole (H*L*) cation and 63% in the picolinate/perchlorate anions. Additionally, H$\cdots$H contacts accounted 33% for thiadiazole (H*L*) cation and 13% for picolinate/perchlorate anions. The FP plots (Fig. 3) further elucidate these contributions. The HS analysis unequivocally reveals that the title compound is primarily consolidated by a network of O—H$\cdots$O hydrogen bonds, which facilitate the formation of an extended three-dimensional supramolecular architecture in the solid state.

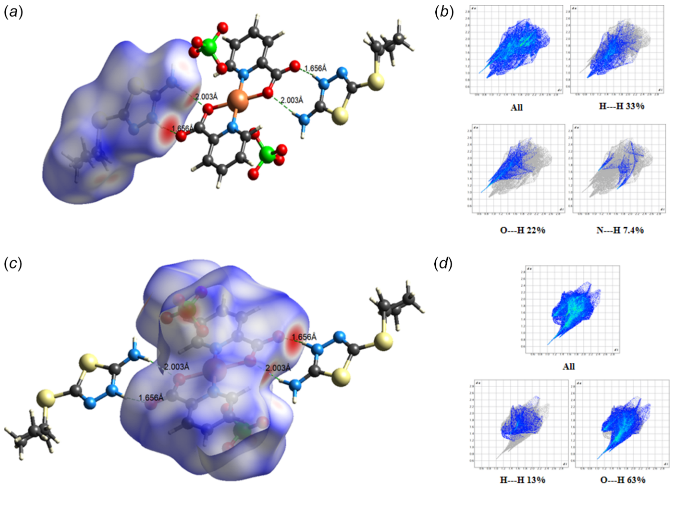

Figure 3
Different views of the Hirshfeld surfaces (*a*) thiadiazole (H*L*) cation, (*b*) two-dimensional fingerprint plots of the H*L* cation, (*c*) picolinate/perchlorate anions and (*d*) two-dimensional fingerprint plots of the sulfate anion and picolinate/perchlorate anions.

5. Database survey

A survey conducted using ConQuest software (CSD, Version 5.46, November 2024; Groom *et al.*, 2016) within the Cambridge Structural Database revealed 311 metal complex crystal structures in which two picolinate anions are coordinated bidentately to a metal center. Among these, only two structures [NEBQAP (Csonka *et al.*, 2018) and TAFNAQ (Guo *et al.*, 2003)] feature a perchlorate anion directly coordinated to a copper(II) atom. Additionally, 22 organometallic crystal structures containing 2-amino-5-mercapto-1,3,4-thiadiazole derivatives have been reported, and in all cases, the thiadiazole ligand binds to the metal through the nitrogen atom at the 3-position [CADMIH (Heidari *et al.*, 2020); CEDSEM (Slyvka, 2017*a*); ESIBUG (Slyvka *et al.*, 2021); FEXPUX (Zou *et al.*, 2023); GAKMOX (Mu *et al.*, 2016); HAJLUC, HAJMAJ and HAJMIR (Ardan *et al.*, 2017); HONDOG (Torambetov *et al.*, 2019); JIYTEU (Gurbanov *et al.*, 2023); JIZKEK and JIZKEK01 (Soudani *et al.*, 2014); JOJLUT (Kadirova *et al.*, 2022); LIFCEK (Hu *et al.*., 2012*a*); LOKYIX (Atashov *et al.*, 2024); ODAPOC (Slyvka *et al.*, 2022); TEGWIN (Hu *et al.*, 2012*b*>); XIGWEQ, XIGWIU, XIGWOA and XIGWUG (Camí *et al.*, 2005); YEBNAX (Slyvka, 2017*b*). Remarkably, no crystal structures have been reported in which the 1,3,4-thiadiazole-based ligand exists in a protonated form and is located in the outer coordination sphere of the complex as a cation. These observations underscore the novelty of the structural motif reported in the present work.

6. Synthesis and crystallization

$Cu(ClO_4)_2·6H_2O$ (0.185 g, 0.5 mmol) and picolinic acid (0.123 g, 1 mmol) were each dissolved separately in methanol (3 mL). The two solutions were then mixed and stirred at 323 K for 1 h. A solution of *L* (2-amino-5-ethylthio-1,3,4-thiadiazole) was prepared by dissolving *L* (0.161 g, 1 mmol) in 3 mL of methanol. This solution was added dropwise to the previously prepared copper(II) perchlorate–picolinic acid solution, resulting in the formation of a blue solution. Upon continuous stirring at 323 K for 4 h, the color of the reaction mixture gradually changed to green. The solution was then filtered and left to crystallize. Single crystals of the title complex, suitable for X-ray diffraction analysis, were obtained by slow evaporation of the filtrate over a period of 7 days.

7. Refinement

Crystal data, data collection and structure refinement details are summarized in Table 2. H atoms were positioned geometrically (N—H = 0.86 Å, C—H = 0.93–0.97 Å) and refined as riding with $U_{\rm iso}$(H) = 1.2$U_{\rm eq}$(N, C) or 1.5$U_{\rm eq}$(C-methyl). The ethyl group of the thiadiazole molecule is disordered over two positions, C9 and C10, with equal occupancies.

Acknowledgements

BT would like to acknowledge the CSIR–TWAS fellowship and the FAIRE programme provided by the Cambridge Crystallographic Data Centre (CCDC) for the use of the Cambridge Structural Database (CSD) and associated software.

Table 2
Experimental details.

Crystal data	
Chemical formula	$(C_4H_8N_3S_2)_2[Cu(C_6H_4NO_2)_2(ClO_4)_2]$
M_r	828.13
Crystal system, space group	Triclinic, $P\overline{1}$
Temperature (K)	299
a, b, c (Å)	6.3100 (2), 9.8179 (2), 13.3493 (4)
α, β, γ (°)	90.522 (1), 98.818 (1), 99.478 (1)
V (Å^3)	805.57 (4)
Z	1
Radiation type	Mo $K\alpha$
μ (mm^{-1})	1.17
Crystal size (mm)	0.11 × 0.1 × 0.06
Data collection	
Diffractometer	Bruker D8 VENTURE Kappa Duo PHOTON II CPAD
Absorption correction	Multi-scan (*SADABS*; Krause *et al.*, 2015)
$T_{\rm min}$, $T_{\rm max}$	0.633, 0.745
No. of measured, independent and observed [$I > 2\sigma(I)$] reflections	28717, 3315, 2937
$R_{\rm int}$	0.057
$(\sin \theta/\lambda)_{\rm max}$ (Å^{-1})	0.628
Refinement	
$R[F^2 > 2\sigma(F^2)]$, $wR(F^2)$, S	0.035, 0.099, 1.03
No. of reflections	3315
No. of parameters	233
No. of restraints	24
H-atom treatment	H-atom parameters constrained
$\Delta\rho_{\rm max}$, $\Delta\rho_{\rm min}$ (e Å^{-3})	0.40, −0.30

Computer programs: *APEX3* and *SAINT* (Bruker, 2016), *SHELXT2018/2* (Sheldrick, 2015*a*), *SHELXL2016/6* (Sheldrick, 2015*b*) and *OLEX2* (Dolomanov *et al.*, 2009).

References

Ardan, B., Kinzhybalo, V., Slyvka, Y., Shyyka, O., Luk‘yanov, M., Lis, T. & Mys‘kiv, M. (2017). *Acta Cryst.* C**73**, 36–46.

Atashov, A., Azamova, M., Ziyatov, D., Uzakbergenova, Z., Torambetov, B., Holczbauer, T., Ashurov, J. & Kadirova, S. (2024). *Acta Cryst.* E**80**, 408–412.

Bernstein, J., Davis, R. E., Shimoni, L. & Chang, N. L. (1995). *Angew. Chem. Int. Ed. Engl.* **34**, 1555–1573.

Bruker (2016). *APEX2* and *SAINT*. Bruker AXS Inc., Madison, Wisconsin, USA.

Camí, G. E., Liu González, M., Sanz Ruiz, F. & Pedregosa, J. C. (2005). *J. Phys. Chem. Solids* **66**, 936–945.

Csonka, R., Lakk-Bogáth, D., Gömöry, Á., Drahos, L., Giorgi, M., Speier, G., Szilágyi, R. K. & Kaizer, J. (2018). *Inorg. Chim. Acta* **472**, 307–319.

Dani, R. K., Bharty, M. K., Prakash, O., Singh, R. K., Prashanth, B., Singh, S. & Singh, N. K. (2015). *J. Coord. Chem.* **68**, 2666–2681.

Dolomanov, O. V., Bourhis, L. J., Gildea, R. J., Howard, J. A. K. & Puschmann, H. (2009). *J. Appl. Cryst.* **42**, 339–341.

Fábry, J. (2018). *Acta Cryst.* E**74**, 1344–1357.

Gond, M. K., Pandey, S. K., Chandra, S., Tiwari, N., Bharty, M. K., Maiti, B., Katiyar, D. & Butcher, R. J. (2022). *J. Mol. Struct.* **1267**, 133586.

Groom, C. R., Bruno, I. J., Lightfoot, M. P. & Ward, S. C. (2016). *Acta Cryst.* B**72**, 171–179.

Guo, G. H., Guo, G. C., Zhou, G. W., Wang, M. S., Cai, L. Z., Wu, A. Q. & Huang, J. S. (2003). *Chin. J. Inorg. Chem.* **19**, 95–98.

Gurbanov, A. V., Aliyeva, V. A., Gomila, R. M., Frontera, A., Mahmudov, K. T. & Pombeiro, A. J. (2023). *Cryst. Growth Des.* **23**, 7335–7344.

Heidari, L., Ghassemzadeh, M., Fenske, D., Fuhr, O., Saeidifar, M. & Mohsenzadeh, F. (2020). *New J. Chem.* **44**, 16769–16775.

Hu, B., Yao, X.-Q., Lu, Y.-Y., Zhou, Y.-M. & Wei, T.-B. (2012). Wuji Huaxue Xuebao, 28, 2581.

Hu, S., Yu, F.., Zhang, P. & Zhou, A.. (2012). *Eur. J. Inorg. Chem.* pp. 3669–3673.

Hu, Y., Li, C. Y., Wang, X. M., Yang, Y. H. & Zhu, H. L. (2014). *Chem. Rev.* **114**, 5572–5610.

Ishankhodzhaeva, M. M., Kadyrova, S. A., Talipov, S. A., Ibragimov, B. T., Fun, K. K., Sundara Razh, S. S. & Parpiev, N. A. (2001). *Russ. J. Gen. Chem.* **71**, 1066–1069.

Kadirova, S., Torambetov, B., Razzokova, S., Uzakbergenova, Z., Abdreymov, A., Raxmonova, D. & Parpiev, N. (2022). *AIP Conf. Proc.* **2471**, 050034.

Karcz, D., Matwijczuk, A., Kamiński, D., Creaven, B., Ciszkowicz, E., Lecka-Szlachta, K. & Starzak, K. (2020). *Int. J. Mol. Sci.* **21**, 5735.

Krause, L., Herbst-Irmer, R., Sheldrick, G. M. & Stalke, D. (2015). *J. Appl. Cryst.* **48**, 3–10.

Lavrenova, L. G., Sukhikh, T. S., Glinskaya, L. A., Trubina, S. V., Zvereva, V. V., Lavrov, A. N., Klyushova, L. S. & Artem’ev, A. V. (2023). *Int. J. Mol. Sci.* **24**, 13024.

Ma, Y., Mu, B. & Huang, R. D. (2018). *Transit. Met. Chem.* **43**, 103–113.

Mu, B., Wang, Q. & Huang, R. (2016). *RSC Adv.* **6**, 12114–12122.

Nuralieva, G., Alieva, M., Torambetov, B., Christopher Leslee, D. B., Senthilkumar, B., Kaur, S., Dabke, N. D., Vanka, K., Ashurov, J., Kadirova, Sh. & Gonnade, R. (2025). *J. Mol. Struct.* **1338**, 142274.

Sheldrick, G. M. (2015*a*). *Acta Cryst.* A**71**, 3–8.

Sheldrick, G. M. (2015*b*). *Acta Cryst.* C**71**, 3–8.

Shen, X. Q., Zhong, H. J., Zheng, H., Zhang, H. Y., Zhao, G. H., Wu, Q. A., Mao, H., Wang, E. & Zhu, Y. (2004). *Polyhedron* **23**, 1851–1857.

Slyvka, Y. (2017*a*). *Visnyk Lviv Univ. Ser. Chem.* **58**, 172.

Slyvka, Y., Kinzhybalo, V., Shyyka, O. & Mys’kiv, M. (2021). *Acta Cryst.* C**77**, 249–256.

Slyvka, Y. I. (2017*b*). *J. Struct. Chem.* **58**, 356–357.

Slyvka, Y. I., Goreshnik, E., Pokhodylo, N. T. & Mys’kiv, M. G. (2022). *J. Chem. Crystallogr.* **52**, 205–213.

Song, Y., Ji, Y.-F., Kang, M.-Y. & Liu, Z.-L. (2012). *Acta Cryst.* E**68**, m772.

Soudani, S., Zeller, M., Wenger, E., Jelsch, C., Lefebvre, F. & Nasr, C. B. (2014). *J. Mol. Struct.* **1075**, 442–449.

Spackman, P. R., Turner, M. J., McKinnon, J. J., Wolff, S. K., Grimwood, D. J., Jayatilaka, D. & Spackman, M. A. (2021). *J. Appl. Cryst.* **54**, 1006–1011.

Torambetov, B., Kadirova, S., Toshmurodov, T., Ashurov, J. M., Parpiev, N. A. & Ziyaev, A. (2019). *Acta Cryst.* E**75**, 1239–1242.

Veidis, M. V., Schreiber, G. H., Gough, T. E. & Palenik, G. J. (1969). *J. Am. Chem. Soc.* **91**, 1859–1860.

Zou, Y., Gao, Q., Sun, N., Han, S., Li, X. & Wang, G. (2023). *Chin. Chem. Lett.* **34**, 107390.

supporting information

Acta Cryst. (2025). E**81**, 613-617   [https://doi.org/10.1107/S2056989025004992]

Synthesis, crystal structure and Hirshfeld surface analysis of bis[2-amino-5-(ethylsulfanyl)-1,3,4-thiadiazol-3-ium] bis(perchlorato-*κO*)bis(picolinato-*κ*^{2}*N*,*O*)copper(II)

Gulnaz Khojabaeva, Batirbay Torambetov, Rajesh G. Gonnade, Zamira Uzakbergenova, Abdusamat Rasulov and Shakhnoza Kadirova

Computing details

Bis[2-amino-5-(ethylsulfanyl)-1,3,4-thiadiazol-3-ium] bis(perchlorato-*κO*)bis(picolinato-*κ*^{2}*N*,*O*)copper(II)

Crystal data

$(C_4H_8N_3S_2)_2[Cu(C_6H_4NO_2)_2(ClO_4)_2]$
$M_r = 828.13$
Triclinic, $P\overline{1}$
$a = 6.3100\ (2)$ Å
$b = 9.8179\ (2)$ Å
$c = 13.3493\ (4)$ Å
$\alpha = 90.522\ (1)°$
$\beta = 98.818\ (1)°$
$\gamma = 99.478\ (1)°$
$V = 805.57\ (4)$ Å^3
$Z = 1$
$F(000) = 420$
$D_x = 1.707$ Mg m^{-3}
Mo $K\alpha$ radiation, $\lambda = 0.71073$ Å
Cell parameters from 9876 reflections
$\theta = 2.6–26.4°$
$\mu = 1.17$ mm^{-1}
$T = 299$ K
Block, green
0.11 × 0.1 × 0.06 mm

Data collection

Bruker D8 VENTURE Kappa Duo PHOTON II CPAD diffractometer
Detector resolution: 7.39 pixels mm^{-1}
φ and ω scans
Absorption correction: multi-scan (SADABS; Krause *et al.*, 2015)
$T_{min} = 0.633$, $T_{max} = 0.745$
28717 measured reflections
3315 independent reflections
2937 reflections with $I > 2\sigma(I)$
$R_{int} = 0.057$
$\theta_{max} = 26.5°$, $\theta_{min} = 2.6°$
$h = -7 \rightarrow 7$
$k = -12 \rightarrow 12$
$l = -16 \rightarrow 16$

Refinement

Refinement on F^2
Least-squares matrix: full
$R[F^2 > 2\sigma(F^2)] = 0.035$
$wR(F^2) = 0.099$
$S = 1.03$
3315 reflections
233 parameters
24 restraints
Hydrogen site location: inferred from neighbouring sites
H-atom parameters constrained
$w = 1/[\sigma^2(F_o^2) + (0.0476P)^2 + 0.4379P]$ where $P = (F_o^2 + 2F_c^2)/3$
$(\Delta/\sigma)_{max} < 0.001$
$\Delta\rho_{max} = 0.40$ e Å^{-3}
$\Delta\rho_{min} = -0.30$ e Å^{-3}

Special details

Geometry. All esds (except the esd in the dihedral angle between two l.s. planes) are estimated using the full covariance matrix. The cell esds are taken into account individually in the estimation of esds in distances, angles and torsion angles; correlations between esds in cell parameters are only used when they are defined by crystal symmetry. An approximate (isotropic) treatment of cell esds is used for estimating esds involving l.s. planes.

Fractional atomic coordinates and isotropic or equivalent isotropic displacement parameters (Å^2)

	x	y	z	$U_{\rm iso}$*/$U_{\rm eq}$	Occ. (<1)
Cu1	0.500000	0.500000	0.000000	0.04229 (13)	
S1	−0.22380 (12)	0.45846 (8)	0.36426 (6)	0.0638 (2)	
S2	−0.33608 (16)	0.66980 (10)	0.50029 (7)	0.0859 (3)	
Cl1	0.55824 (9)	0.20197 (6)	0.16167 (5)	0.05452 (17)	
O1	0.3708 (2)	0.55987 (16)	0.11468 (13)	0.0472 (4)	
O2	0.4332 (3)	0.72184 (19)	0.23898 (14)	0.0593 (5)	
O3	0.7223 (4)	0.1767 (2)	0.24227 (18)	0.0776 (6)	
O4	0.4945 (4)	0.0857 (2)	0.0948 (2)	0.0889 (7)	
O5	0.3737 (4)	0.2359 (3)	0.1990 (2)	0.0906 (7)	
O6	0.6536 (3)	0.3183 (2)	0.10864 (18)	0.0729 (6)	
N3	−0.0062 (4)	0.7053 (2)	0.39137 (18)	0.0620 (6)	
N4	0.0747 (4)	0.4205 (3)	0.24606 (18)	0.0657 (6)	
H4A	0.189153	0.449554	0.219641	0.079*	
H4B	0.008829	0.336685	0.234388	0.079*	
N1	0.7410 (3)	0.65204 (18)	0.05284 (14)	0.0404 (4)	
N2	0.0878 (3)	0.6329 (2)	0.32667 (16)	0.0558 (5)	
H2	0.200239	0.671103	0.301887	0.067*	
C1	0.6886 (3)	0.7281 (2)	0.12672 (16)	0.0400 (4)	
C2	0.8134 (4)	0.8502 (2)	0.16490 (19)	0.0488 (5)	
H2A	0.772326	0.900672	0.215821	0.059*	
C3	1.0027 (4)	0.8970 (3)	0.1258 (2)	0.0541 (6)	
H3	1.089572	0.980444	0.149272	0.065*	
C4	1.0600 (4)	0.8186 (3)	0.0522 (2)	0.0521 (6)	
H4	1.188109	0.847296	0.026328	0.063*	
C5	0.9263 (3)	0.6967 (2)	0.01687 (18)	0.0471 (5)	
H5	0.965821	0.643983	−0.033273	0.057*	
C6	0.4818 (4)	0.6673 (2)	0.16415 (17)	0.0434 (5)	
C7	0.0006 (4)	0.5040 (3)	0.30408 (18)	0.0503 (5)	
C8	−0.1698 (4)	0.6261 (3)	0.4178 (2)	0.0572 (6)	
C9	−0.218 (3)	0.8510 (10)	0.5248 (9)	0.089 (3)	0.5
H9B	−0.063195	0.856523	0.546730	0.106*	0.5
H9A	−0.236435	0.897343	0.460917	0.106*	0.5
C10	−0.299 (2)	0.9253 (9)	0.5957 (8)	0.124 (4)	0.5
H10A	−0.232139	1.020680	0.596917	0.186*	0.5
H10B	−0.265597	0.888642	0.661633	0.186*	0.5
H10C	−0.453377	0.917710	0.577437	0.186*	0.5
C9A	−0.297 (3)	0.869 (2)	0.4976 (17)	0.180 (9)	0.5
H9AA	−0.241457	0.906202	0.437962	0.215*	0.5
H9AB	−0.424855	0.906473	0.508259	0.215*	0.5

C10A	−0.135 (3)	0.878 (2)	0.5860 (14)	0.169 (6)	0.5

Atomic displacement parameters (Å^2)

	U^{11}	U^{22}	U^{33}	U^{12}	U^{13}	U^{23}
Cu1	0.0311 (2)	0.0428 (2)	0.0522 (2)	−0.00334 (14)	0.01479 (15)	−0.00666 (16)
S1	0.0555 (4)	0.0684 (4)	0.0696 (4)	−0.0064 (3)	0.0344 (3)	−0.0101 (3)
S2	0.0874 (6)	0.0956 (6)	0.0854 (6)	0.0158 (5)	0.0478 (5)	−0.0145 (5)
Cl1	0.0440 (3)	0.0499 (3)	0.0709 (4)	0.0048 (2)	0.0168 (3)	−0.0048 (3)
O1	0.0375 (8)	0.0445 (8)	0.0598 (9)	−0.0041 (6)	0.0203 (7)	−0.0047 (7)
O2	0.0535 (10)	0.0640 (11)	0.0612 (10)	−0.0048 (8)	0.0277 (8)	−0.0129 (8)
O3	0.0809 (14)	0.0635 (12)	0.0845 (14)	0.0103 (10)	0.0026 (11)	0.0113 (10)
O4	0.0774 (15)	0.0731 (14)	0.1099 (18)	−0.0060 (11)	0.0173 (13)	−0.0357 (13)
O5	0.0708 (14)	0.0922 (16)	0.123 (2)	0.0205 (12)	0.0520 (14)	0.0009 (14)
O6	0.0512 (11)	0.0727 (12)	0.0931 (15)	0.0042 (9)	0.0114 (10)	0.0221 (11)
N3	0.0627 (14)	0.0594 (13)	0.0663 (14)	0.0038 (10)	0.0249 (11)	−0.0047 (10)
N4	0.0539 (13)	0.0712 (14)	0.0735 (15)	−0.0049 (11)	0.0320 (11)	−0.0152 (12)
N1	0.0308 (8)	0.0420 (9)	0.0477 (10)	0.0006 (7)	0.0104 (7)	−0.0008 (7)
N2	0.0483 (11)	0.0608 (12)	0.0595 (12)	0.0003 (9)	0.0222 (10)	0.0002 (10)
C1	0.0336 (10)	0.0408 (10)	0.0459 (11)	0.0036 (8)	0.0104 (8)	0.0037 (9)
C2	0.0479 (13)	0.0439 (12)	0.0541 (13)	0.0015 (9)	0.0137 (10)	−0.0053 (10)
C3	0.0463 (13)	0.0447 (12)	0.0662 (15)	−0.0089 (10)	0.0115 (11)	−0.0027 (11)
C4	0.0361 (11)	0.0539 (13)	0.0639 (14)	−0.0057 (9)	0.0147 (10)	0.0025 (11)
C5	0.0343 (11)	0.0526 (12)	0.0543 (13)	0.0006 (9)	0.0143 (9)	−0.0026 (10)
C6	0.0379 (11)	0.0455 (11)	0.0484 (12)	0.0040 (9)	0.0152 (9)	0.0027 (9)
C7	0.0390 (12)	0.0634 (14)	0.0485 (12)	0.0019 (10)	0.0143 (10)	−0.0012 (10)
C8	0.0541 (14)	0.0659 (15)	0.0543 (14)	0.0088 (12)	0.0187 (11)	−0.0031 (12)
C9	0.127 (7)	0.068 (4)	0.079 (5)	0.030 (4)	0.030 (5)	−0.018 (4)
C10	0.186 (10)	0.082 (5)	0.125 (7)	0.023 (6)	0.089 (7)	−0.013 (5)
C9A	0.159 (12)	0.198 (12)	0.192 (12)	0.038 (8)	0.054 (8)	−0.039 (8)
C10A	0.175 (12)	0.194 (13)	0.141 (11)	0.025 (11)	0.041 (10)	0.023 (10)

Geometric parameters (Å, º)

Cu1—O1$^{\rm i}$	1.9693 (15)	N1—C5	1.341 (3)
Cu1—O1	1.9693 (15)	N2—H2	0.8600
Cu1—N1	1.9854 (17)	N2—C7	1.307 (3)
Cu1—N1$^{\rm i}$	1.9854 (17)	C1—C2	1.368 (3)
S1—C7	1.731 (2)	C1—C6	1.503 (3)
S1—C8	1.748 (3)	C2—H2A	0.9300
S2—C8	1.730 (3)	C2—C3	1.387 (3)
S2—C9	1.818 (10)	C3—H3	0.9300
S2—C9A	1.93 (2)	C3—C4	1.369 (4)
Cl1—O3	1.428 (2)	C4—H4	0.9300
Cl1—O4	1.408 (2)	C4—C5	1.379 (3)
Cl1—O5	1.421 (2)	C5—H5	0.9300
Cl1—O6	1.444 (2)	C9—H9B	0.9700
O1—C6	1.281 (3)	C9—H9A	0.9700

O2—C6	1.231 (3)	C9—C10	1.394 (12)
N3—N2	1.374 (3)	C10—H10A	0.9600
N3—C8	1.284 (3)	C10—H10B	0.9600
N4—H4A	0.8600	C10—H10C	0.9600
N4—H4B	0.8600	C9A—H9AA	0.9700
N4—C7	1.310 (3)	C9A—H9AB	0.9700
N1—C1	1.344 (3)	C9A—C10A	1.43 (2)

O1^{i}—Cu1—O1	180.0	C4—C3—H3	120.4
O1—Cu1—N1^{i}	97.01 (7)	C3—C4—H4	120.3
O1—Cu1—N1	82.99 (7)	C3—C4—C5	119.5 (2)
O1^{i}—Cu1—N1^{i}	82.99 (7)	C5—C4—H4	120.3
O1^{i}—Cu1—N1	97.01 (7)	N1—C5—C4	121.8 (2)
N1^{i}—Cu1—N1	180.0	N1—C5—H5	119.1
C7—S1—C8	87.51 (12)	C4—C5—H5	119.1
C8—S2—C9	99.3 (4)	O1—C6—C1	115.90 (19)
C8—S2—C9A	103.8 (7)	O2—C6—O1	125.3 (2)
O3—Cl1—O6	106.67 (13)	O2—C6—C1	118.8 (2)
O4—Cl1—O3	110.34 (15)	N4—C7—S1	124.9 (2)
O4—Cl1—O5	109.73 (15)	N2—C7—S1	110.12 (18)
O4—Cl1—O6	109.64 (16)	N2—C7—N4	125.0 (2)
O5—Cl1—O3	111.56 (16)	S2—C8—S1	118.33 (16)
O5—Cl1—O6	108.82 (14)	N3—C8—S1	115.4 (2)
C6—O1—Cu1	114.18 (13)	N3—C8—S2	126.3 (2)
C8—N3—N2	109.2 (2)	S2—C9—H9B	107.8
H4A—N4—H4B	120.0	S2—C9—H9A	107.8
C7—N4—H4A	120.0	H9B—C9—H9A	107.1
C7—N4—H4B	120.0	C10—C9—S2	118.0 (9)
C1—N1—Cu1	111.77 (13)	C10—C9—H9B	107.8
C5—N1—Cu1	129.29 (15)	C10—C9—H9A	107.8
C5—N1—C1	118.30 (19)	C9—C10—H10A	109.5
N3—N2—H2	121.1	C9—C10—H10B	109.5
C7—N2—N3	117.7 (2)	C9—C10—H10C	109.5
C7—N2—H2	121.1	H10A—C10—H10B	109.5
N1—C1—C2	122.9 (2)	H10A—C10—H10C	109.5
N1—C1—C6	114.28 (18)	H10B—C10—H10C	109.5
C2—C1—C6	122.8 (2)	S2—C9A—H9AA	113.7
C1—C2—H2A	120.8	S2—C9A—H9AB	113.7
C1—C2—C3	118.4 (2)	H9AA—C9A—H9AB	110.9
C3—C2—H2A	120.8	C10A—C9A—S2	89.9 (15)
C2—C3—H3	120.4	C10A—C9A—H9AA	113.7
C4—C3—C2	119.1 (2)	C10A—C9A—H9AB	113.7

Cu1—O1—C6—O2	−179.2 (2)	C2—C3—C4—C5	1.5 (4)
Cu1—O1—C6—C1	−0.1 (2)	C3—C4—C5—N1	−0.2 (4)
Cu1—N1—C1—C2	−170.09 (18)	C5—N1—C1—C2	1.6 (3)
Cu1—N1—C1—C6	10.1 (2)	C5—N1—C1—C6	−178.19 (19)
Cu1—N1—C5—C4	168.70 (18)	C6—C1—C2—C3	179.4 (2)

N3—N2—C7—S1	0.7 (3)	C7—S1—C8—S2	−178.53 (18)
N3—N2—C7—N4	−178.0 (3)	C7—S1—C8—N3	1.2 (2)
N1—C1—C2—C3	−0.3 (4)	C8—S1—C7—N4	177.7 (3)
N1—C1—C6—O1	−6.9 (3)	C8—S1—C7—N2	−1.0 (2)
N1—C1—C6—O2	172.3 (2)	C8—S2—C9—C10	−175.6 (12)
N2—N3—C8—S1	−1.0 (3)	C8—N3—N2—C7	0.2 (3)
N2—N3—C8—S2	178.7 (2)	C9—S2—C8—S1	−176.8 (5)
C1—N1—C5—C4	−1.3 (3)	C9—S2—C8—N3	3.5 (6)
C1—C2—C3—C4	−1.2 (4)	C9A—S2—C8—S1	−158.3 (6)
C2—C1—C6—O1	173.3 (2)	C9A—S2—C8—N3	22.0 (7)
C2—C1—C6—O2	−7.5 (3)		

Symmetry code: (i) −*x*+1, −*y*+1, −*z*.

Hydrogen-bond geometry (Å, º)

D—H···*A*	*D*—H	H···*A*	*D*···*A*	*D*—H···*A*
N4—H4*A*···O1	0.86	2.14	2.940 (3)	156
N4—H4*A*···O5	0.86	2.59	2.951 (3)	106
N4—H4*B*···O3^{ii}	0.86	2.21	2.981 (3)	150
N4—H4*B*···O6^{ii}	0.86	2.57	3.005 (3)	113
N2—H2···O2	0.86	1.81	2.656 (3)	170

Symmetry code: (ii) *x*−1, *y*, *z*.